Atmos. Chem. Phys. Discuss., 5, 9355–9404, 2005
www.atmos-chem-phys.org/acpd/5/9355/
SRef-ID: 1680-7375/acpd/2005-5-9355
European Geosciences Union

Atmospheric Chemistry and Physics Discussions

Spectral light absorption by ambient aerosols influenced by biomass burning in the Amazon Basin – I. Comparison and field calibration of absorption measurement techniques

O. Schmid[1,6], P. Artaxo[2], W. P. Arnott[3], D. Chand[1], L. V. Gatti[4], G. P. Frank[1], A. Hoffer[1], M. Schnaiter[5], and M. O. Andreae[1]

[1]Max Planck Institute for Chemistry, Department of Biogeochemistry, PO Box 3060, 55020 Mainz, Germany
[2]University of São Paulo, Institute of Physics, São Paulo, Brazil
[3]Desert Research Institute, Division of Atmospheric Science, Reno, NV, USA
[4]Institute of Nuclear Energy Research, Atmospheric Chemistry Laboratory, São Paulo, SP, Brazil
[5]Research Center Karlsruhe, Institute of Meteorology and Climate Research, PO Box 3640, 76021 Karlsruhe, Germany

[6] now at: GSF – National Research Center for Environment and Health, Institute for Inhalation Biology, PO Box 1129, 85758 Neuherberg/Munich, Germany

Received: 11 July 2005 – Accepted: 24 August 2005 – Published: 29 September 2005

Correspondence to: O. Schmid (oschmid@mpch-mainz.mpg.de)

Abstract

Spectral aerosol light absorption is an important parameter for the assessment of the radiation budget of the atmosphere. Although on-line measurement techniques for aerosol light absorption, such as the Aethalometer and the Particle Soot Absorption Photometer (PSAP), have been available for two decades, they are limited in accuracy and spectral resolution because of the need to deposit the aerosol on a filter substrate before measurement. Recently, a 7-wavelength (λ) Aethalometer became commercially available, which covers the visible (VIS) to near-infrared (NIR) spectral range (λ=450–950 nm), and laboratory calibration studies improved the degree of confidence in these measurement techniques. However, the applicability of the laboratory calibration factors to ambient conditions has not been investigated thoroughly yet.

As part of the LBA-SMOCC (Large scale Biosphere atmosphere experiment in Amazonia – SMOke aerosols, Clouds, rainfall and Climate) campaign from September to November 2002 in the Amazon basin we performed an extensive field calibration of a 1-λ PSAP and a 7-λ Aethalometer utilizing a photoacoustic spectrometer (PAS, 532 nm) as reference device. Especially during the dry period of the campaign, the aerosol population was dominated by pyrogenic emissions. The most pronounced artifact of integrating-plate type attenuation techniques is due to multiple scattering effects within the filter matrix. For the PSAP, we essentially confirmed the laboratory calibration factor by Bond (1999). On the other hand, for the Aethalometer we found a multiple scattering enhancement of 5.23 (or 4.55, if corrected for aerosol scattering), which is significantly larger than the factors previously reported (~2). While the exact reason for this discrepancy is unknown, the available data from the present and previous studies suggest aerosol mixing (internal versus external) as a likely cause. While it is well-known that RH may (moderately) affect aerosol absorption, we found no dependence of either PSAP or Aethalometer on relative humidity (RH) for 30%<RH<55% and 40%<RH<80%, respectively. However, a substantial decrease in PSAP sensitivity was observed for low RH (20%<RH<30%). In addition, while the PSAP demon-

ACPD

5, 9355–9404, 2005

strated no sensitivity to gaseous adsorption, the Aethalometer response was clearly positively correlated with the gradient in pollution level. Hence, although very similar in measurement principle, the PSAP and Aethalometer require markedly different correction factors, which is probably due to the different filter media used. Although on-site calibration of the PSAP and Aethalometer is suggested for best data quality, we recommend a set of PSAP and Aethalometer correction factors for ambient sampling based on the data from the present and previous studies. For this study, the estimated accuracies of the absorption coefficients determined by the PAS, PSAP and Aethalometer were 10, 15 and 20%, respectively.

1. Introduction

The Intergovernmental Panel on Climate Change (Penner et al., 2001) has identified radiative forcing by aerosols as one of the major uncertainties in the global radiation budget. While light scattered by aerosols cools the atmosphere (negative radiative forcing), absorbed electromagnetic radiation contributes to a positive radiative forcing. In addition to the direct heating of the atmosphere due to light absorption, there is a semi-direct effect as a result of the enhanced dissipation of clouds in the vicinity of heated aerosol layers (Ackerman et al., 2000; Penner et al., 2001). The latter may have significant implications on regional and global precipitation patterns. Despite its significance, light absorption by atmospheric aerosol is relatively poorly characterized in part due to a lack of reliable instrumentation.

Aerosol light scattering and absorption can be characterized by the scattering and absorption coefficients, σ_s and σ_a, respectively, which describe the attenuation of light per distance and are therefore given in units of inverse meter (or here inverse megameter 1 Mm^{-1}=10^{-6} m^{-1}). For aerosols in the diameter range of between 10 nm and ~10 μm, as considered here, both σ_s and σ_a are complex functions of particle size and shape as well as the degree and kind of mixing with other particles (internally and externally mixed) (Bohren and Huffman, 1983; Fuller et al., 1999). While reliable

ACPD
5, 9355–9404, 2005

in-situ measurement techniques for light scattering by aerosols have been available for several decades (Heintzenberg and Charlson, 1996), light absorption is by nature a more elusive property, since during the absorption process photons are converted into thermal energy, which makes it impossible to detect them directly. Historically, two main (indirect) approaches have been applied to experimentally determine σ_a based on optical and thermal methods, respectively. The optical approach involves the measurement of light attenuation by an aerosol sample with corrections for the effects of light scattering and filter-particle interaction, if applicable. The thermal methods infer σ_a from the absorption-induced heating of the aerosols. The optical approach includes the integrating sphere, plate, and sandwich method as well as their continuous flow versions, the Aethalometer™ (Hansen et al., 1984) and Particle Soot Absorption Photometer (PSAP) (Bond et al., 1999). In addition to these substrate-based methods, there is the so-called difference method, which determines light absorption of particles in their suspended state from the difference of light extinction and scattering. The most prominent representative of the thermal methods is the photoacoustic spectrometer (PAS) (Truex and Anderson, 1979), which infers σ_a from the thermal expansion due to light absorption by suspended particles. While the PSAP, Aethalometer and PAS will be discussed below, we refer to the review papers by Horvath (1993) and McMurry (2000) for details on the other methods.

Historically, aerosol light absorption measurements were most frequently performed with filter-based methods, especially after online versions such as the Aethalometer and PSAP became commercially available in the mid 80s. Laboratory calibrations have provided empirical correction factors for Aethalometer and PSAP instrument artifacts, which are mainly due to filter-substrate interactions (multiple scattering, filter loading) and aerosol scattering (Petzold et al., 1997; Arnott et al., 2005). However, several studies have demonstrated the need for site-specific calibration factors, since filter-based attenuation coefficients depend among other factors on size distribution and mixing state of the aerosol (Liousse et al., 1993; Petzold et al., 1997; Ballach et al., 2001; Arnott et al., 2005). Recently, Petzold and Schönlinner (2004) have ad-

ACPD
5, 9355–9404, 2005

dressed these shortcomings by introducing an advanced version of the Aethalometer, the multiangle absorption photometer (MAAP), that measures not just light transmission (as the Aethalometer and PSAP) but also angular reflection from an aerosol-laden filter (Petzold et al., 2005).

The difference method has frequently been used as reference method for aerosol absorption measurements, since the measurement is performed on particles in their suspended state and the measurement parameters involved are relatively accurately known (length of optical extinction cell, light intensity, and σ_s). Although the difference method has been used for field calibrations in the past (Reid et al., 1998), the instrument is relatively long and the measurements were typically limited to high pollution events due to sensitivity limits. In addition, large uncertainties are introduced into the difference method for typical ambient aerosols with single scattering albedos larger than ~0.8, since in this case absorption is determined from the difference of two large but almost equal numbers (extinction and scattering coefficient) (Schnaiter et al., 2005). Hence, for the field calibration reported here we chose a photoacoustic spectrometer (PAS, λ=532 nm) (Moosmüller et al., 1998; Arnott et al., 1999, 2000, 2003) as reference method. Recent laboratory calibration experiments with kerosene- and spark-generated soot have shown excellent agreement (better than 10%) of this type of PAS with the difference method (Schnaiter et al., 2005; Sheridan et al., 2005; Virkkula et al., 2005b). In addition, the PAS can be calibrated on-site with NO_2 as calibration gas (Arnott et al., 2000).

This study is the first of two parts on spectral light absorption by ambient aerosols in the Amazon Basin measured during the SMOCC field campaign from 9 September to 14 November 2002. Part I reports on the field intercomparison of a 7-λ Aethalometer (λ=450 to 950 nm) and a 1-λ PSAP (565 nm) with a photoacoustic spectrometer (PAS, 532 nm) as reference device. The principle, operation and performance of all three absorption instruments are discussed and the multiple scattering and filter loading correction for the Aethalometer and PSAP are determined. Finally, for the latter two devices, the effects of relative humidity, single scattering albedo and gaseous ad-

ACPD
5, 9355–9404, 2005

sorption onto the filter substrate are investigated. A detailed discussion of the spectral absorption properties of Amazonian aerosol will be provided in the Part 2 of this paper.

2. Experimental

2.1. Measurement site and period

From 9 September to 14 November 2002 the Large Scale Biosphere-Atmosphere Experiment in Amazonia – Smoke, Aerosols, Clouds, Rainfall and Climate (LBA-SMOCC) campaign was conducted in the state of Rondônia, Brazil (Andreae et al., 2004). The measurement station was located on the Fazenda Nossa Senhora Aparecida (FNS, 10.76° S, 62.32° W, 315 m a.s.l.) a pasture site in the south-western part of the Amazon Basin about 50 km north-west of Ji-Parana (10.88° S, 61.85° W, 235 m a.s.l.; ~110 000 inhabitants) (Andreae et al., 2002). While the area around FNS is predominantly grassland, the site is affected by the widespread vegetation fires due to fire-assisted land-clearing activities in the Amazon Basin during the dry season (June–October). The measurement period was selected such that both dry season and wet season data could be collected. Here we will distinguish between three periods: the dry period from 9 September to 8 October (end of dry season), a transition period from 9 October to 30 October, and the wet period from 1 November to 14 November (beginning of wet season). While the dry period is heavily influenced by biomass burning events, this burning signature is significantly reduced in the transition period and reaches even lower levels in the wet season.

2.2. Setup

A comprehensive suite of aerosol, gas phase and meteorological parameters was measured during the SMOCC campaign. Here we focus on instrumentation for aerosol light absorption measurements. As mentioned above, aerosol light absorption was measured with three different instruments: a photoacoustic spectrometer (PAS, λ=532 nm),

ACPD
5, 9355–9404, 2005

a Particle Soot Absorption Photometer (PSAP, Radiance Research, 565 nm) and a 7-λ Aethalometer (AE30, Magee Scientific, 450 to 950 nm). In addition, two integrating nephelometers (λ=545 nm; Radiance Research, M903) were used to measure aerosol light scattering (Chand et al., 2005).

The aerosol inlets (Rupprecht & Patashnick; inlet for the TEOM 1400) were located ~1 m above the roof top of the instrument hut (~7 m above the ground). They were equipped with a 1.5 or 10 μm impactor, i.e., we sampled particulate matter either below 1.5 or 10 μm aerodynamic diameter (PM1.5 and PM10, respectively).

The PSAP, PAS and one of the Radiance Research nephelometers (M903) were sampling from the same Rupprecht & Patashnick PM10 inlet equipped with an additional 1.5 μm impactor. Prior to particle detection the aerosol was dried to RH<45% by a Nafion membrane counter-flow drier (Permapure, Inc.) and then passed through the 1.5 μm impactor. The sampling flow rates of the PSAP, PAS and nephelometer were 0.2–0.4, 0.8 and 1.0–1.2 L min^{-1}, respectively. Although the flow rates for the PSAP and nephelometer are smaller than specified by the manufacturer (to allow for more efficient drying of the sample flow and longer lifetime of the PSAP filter), we have not seen a systematic change in instrument response when the flow rate was increased to manufacturer specifications (PSAP: 1 to 4 L min^{-1}; nephelometer: 10 L min^{-1}).

The particle loss in the Nafion drier (<5% for 50 nm <D_p<700 nm) and the cut-off characteristics of the 1.5 μm impactor were experimentally determined after the campaign with dry ammonium sulphate particles. Both σ_a and σ_s were corrected for line losses (on average ~2.5%) utilizing the measured particle loss, the dry particle size distributions and the Mie code described by Guyon et al. (2003a). Particle loss in the connecting stainless steel transport lines was considered negligible in the size range of interest for aerosol optical properties (30 nm to 10 μm diameter), since for each instrument the length of the connecting tubing was below 10 m and the flow conditions were kept laminar. All flow rates were regularly calibrated to an estimated accuracy of about 2% with a positive displacement flow meter.

The Aethalometer and the other Radiance Research nephelometer were oper-

ated under ambient conditions with a 10 μm cut-off diameter at a flow rate of about 6.6 L min^{-1} and 7 L min^{-1}, respectively. We will refer to these operating conditions as 'ambient', although the term 'non-dried' is more accurate, since although the sample air was not passed through a drier, the operational relative humidity (RH) was somewhat lower than ambient RH due to the slightly elevated instrument temperature, especially during nighttime. While during the relatively dry and warm daytime conditions ambient and instrument RH were within a few percent, the differences reached about 20% during nighttime when ambient RH was close to 100%, but instrument RH only reached about 80%.

Since the Aethalometer and the PAS were operated under different RH conditions and from inlets with different cut-off diameters (PAS: 1.5 μm; Aethalometer: 10 μm), we have to consider these differences when comparing the Aethalometer with the PAS. The effect of RH in Aethalometer performance is negligible as will be discussed below. Regarding the size cut-off we utilized the size-segregated aerosol mass information provided by a collocated MOUDI impactor (Marple et al., 1991). The relative mass contribution of the 1.8 to 10 μm size segment (stage 2+3 of the MOUDI impactor) to PM10 (stages 2 to 10) was on average 7.6% (dry period) and 14.9% (transition period). Considering that most of the absorbing material (black carbon) is found in PM1.5 and that the mass specific absorption cross section α_a (m^2 g^{-1}) decreases with size for supermicron particles (Horvath, 1993), the cut-off-related systematic difference between Aethalometer and PAS signal is expected to be considerably less than 8 and 15% for the dry and intermediate period, respectively. We will see below that a less than 8% difference is negligible compared to other effects. Since the PSAP and PAS were operated from the same inlet, no such considerations are necessary for the PSAP. Unless stated otherwise, all data are referenced to 1000 hPa and 298.2 K.

ACPD
5, 9355–9404, 2005

2.3. Photoacoustic spectrometer (PAS)

2.3.1. Principle of operation

The photoacoustic spectrometer (PAS) determines aerosol light absorption by converting the absorbed energy into an acoustic wave detected by a sensitive microphone (Terhune and Anderson, 1977). While passing aerosol through an acoustic resonator, a power-modulated laser periodically heats the aerosol, which leads to periodic thermal expansions and hence pressure pulses (acoustic wave). Using a calibrated microphone the pressure amplitude P_m of this acoustic wave is measured and the nominal absorption coefficient $\sigma_{\mathrm{PAS,raw}}$ can be calculated according to (Rosencwaig, 1980)

$$\sigma_{\mathrm{PAS,raw}} = P_m \frac{\pi^2 A_{\mathrm{res}} f_0}{P_L \tilde{Q} (\gamma - 1)}, \quad (1)$$

where A_{res}, f_0, and $\tilde{Q}$ are the cross sectional area, the acoustic resonance frequency, and the quality factor of the resonator, respectively, and P_L and γ are the modulated average laser power and the ratio of the isobaric and isochoric specific heats of the carrier gas (γ_{air}=1.4), respectively.

2.3.2. Technical details

The device used here, a refined version of the PAS described by Arnott et al. (1999), was optimized for atmospheric applications by maximizing the signal to noise ratio. The PAS utilizes a frequency-doubled diode-laser-pumped Nd:YAG laser (λ=532 nm), which is power-modulated by a chopper at the resonance frequency of the acoustic resonator (f_0=1500 Hz). The modulated laser power of $P_L \cong$60 mW is continuously monitored (after passing through the resonator) by a photodiode mounted on an integrating sphere. The length (L) and cross-sectional area (A_{res}) of the resonator are 24.86 cm and 2.18 cm^2, respectively. To avoid potential systematic errors due to temperature and pressure drifts in f_0 and $\tilde{Q}$(~75), both f_0 and $\tilde{Q}$ are continuously measured

ACPD
5, 9355–9404, 2005

and optimized for acoustic resonance utilizing a piezoelectric disc. Since P_m, P_L, f_0 and $\tilde{Q}$ are directly measured by the PAS, all parameters of Eq. (1) are known and the absorption coefficient can be calculated without any device-specific calibration factor as typical for most filter-based absorption techniques. From the experimental uncertainties in these measurement parameters we estimated the overall uncertainty of $\sigma_{\mathrm{PAS,raw}}$ as 5%. To optimize the signal to noise ratio (and hence the lower detection limit) the acoustic noise was minimized passively by using absorbing materials, avoiding turbulent flow conditions and sharp bends in the connecting tubing, installing an acoustic filter at the inlet of the resonator (two volumes with different acoustic resonance frequency, i.e., low and high pass filters in series) and isolating the sample pump from the resonator by a critical orifice. It is also noteworthy that, while the sample flow rate (here 0.8 L min^{-1}) affects the response time of the PAS (here: <10 s), it does not enter Eq. (1), i.e., the sample flow rate is irrelevant for the accuracy of the measured σ_a.

2.3.3. Calibration and intercomparison with difference method

As mentioned above, photoacoustic sensors can be calibrated utilizing the well-known absorption properties of gaseous components. While theoretically the gas concentration and its absorption cross-section could be used, Arnott et al. (2000) have introduced an alternative calibration procedure, which does not require this information, in fact does not require any information beyond the data stream provided by the PAS itself. According to this procedure one alternatingly supplies the PAS with clean air and NO_2 (or any other gas which absorbs at the wavelength of the PAS, here 532 nm) and determines the laser light attenuation through the acoustic resonator according to Lambert-Beer's law

$$P_L = P_{L,0} \exp\left(-\sigma_{LB} L\right), \tag{2}$$

where L (=0.2486 m) is the optical length of the resonator, P_L and $P_{L,0}$ are the measured laser intensities with and without NO_2 in the resonator, respectively, and σ_{LB} is the reference absorption value to be determined, which is completely independent of

the photoacoustic signal. It is evident from Eq. (2) that neither the concentration nor the absorption cross section of the calibration gas is required. The only requirement is that σ_{LB} is large enough to introduce a measurable change in P_L and small enough not to exceed the linear response range of the microphone. For the SMOCC campaign, we used ~1000 ppm of NO_2 in synthetic air as calibration gas, which corresponded to an absorption coefficient of $\sigma_{PAS,raw}$ ~320 000 Mm^{-1}. By progressively diluting the calibration gas with filtered air, we confirmed that the microphone was linear up to at least 320 000 Mm^{-1}, i.e., over more than five orders of magnitude.

Figure 1 illustrates a PAS calibration cycle. When the particle free air is replaced by the calibration gas (at measurement point 10), the photoacoustically determined absorption coefficient ($\sigma_{PAS,raw}$; see Eq. 1) increases abruptly from 0.5±1.2 Mm^{-1} to 330 000±3000 Mm^{-1} (average and standard deviation), while the laser intensity (after passing through the resonator) decreases from $P_{L,0}$=61.631±0.009 mW to P_L=56.870±0.014 mW, which according to Eq. (2) corresponds to σ_{LB}=323 000±1000 Mm^{-1}. When at measurement point 24 the PAS is purged with particle free air again, both $\sigma_{PAS,raw}$ and P_L return to their initial conditions. Comparing $\sigma_{PAS,raw}$ and σ_{LB} we find that $\sigma_{PAS,raw}$ is 2.2% larger than σ_{LB} (at a precision of 1.0%), which is well within the estimated overall uncertainty of the PAS (5%). Again we mention that this simple two-point calibration procedure does not rely on any external calibration standard nor does it require exact knowledge of the NO_2 concentration or any other information not provided by the PAS. As an additional measure of quality assurance we performed a laboratory intercomparison of the PAS with the difference method for various types of aerosols. The difference method utilized an optical extinction cell, the Long Path Optical Extinction Spectrometer (LOPES), and an integrating nephelometer (TSI, model 3563), where the scattering data were corrected for nephelometer errors due to angular truncation and non-Lambertian light source as described by Schnaiter et al. (2005). Figure 2 depicts the measured absorption coefficients for pure soot particles (solid symbols) and soot particles coated with non-absorbing materials (organic and inorganic; open symbols), where the organic coat-

ACPD
5, 9355–9404, 2005

ing was produced by ozonolysis of α-pinene, which among other organic compounds generates pinic and pinonic acids (Saathoff et al., 2003). The absorption coefficients measured by the PAS and the optical extinction cell agree well for both pure soot particles (Diesel and spark-generated [Palas] soot) and coated soot particles (slope = 0.972±0.022). This confirms the results from a previous laboratory study which was performed on pure soot and biomass burning aerosols (Schnaiter et al., 2005).

2.3.4. Data reduction and accuracy

The main sources for systematic uncertainties of the PAS under field conditions are zero point instabilities and the cross-sensitivity to ambient NO_2. Since this results in a potentially variable zero-point offset, the instrument offset was repeatedly determined by zero calibrations using filtered (particle-free) ambient air for 10 to 30 min (at least) twice a day. We corrected for the NO_2 cross-sensitivity utilizing the ambient NO_2 mixing ratio continuously measured by a Model 42CTL NO/NO_x monitor (Thermo Environment Instruments Inc.) (Kirkman et al., 2002). For the same Nd:YAG laser as used here, Arnott et al. (2000) determined a NO_2 specific absorption coefficient of 0.306±0.015 Mm^{-1} ppb^{-1} (156 000±1000 Mm^{-1} for 509 000±25 000 ppb of NO_2) at 846 hPa and 294.7 K. Hence, the NO_2-induced PAS offset can be expressed as

$$\sigma_{NO2} = 0.306 \frac{p}{846\,\mathrm{hPa}} \frac{294.7\,\mathrm{K}}{T} c_{NO2}\mathrm{Mm^{-1}ppb^{-1}} = B_{NO2}\frac{p}{T}c_{NO2}, \quad (3)$$

where the lump constant B_{NO2} equals 0.107±0.005 K hPa^{-1} ppb^{-1} Mm^{-1} and p, T and c_{NO2} are the operating pressure, temperature and NO_2 (volume) mixing ratio, respectively. Based on these considerations the PAS data was corrected for each time layer for zero offset and NO_2 sensitivity according to

$$\sigma_{PAS} = \sigma_{PAS,raw} - \sigma_0 - B_{NO2}\left(\frac{p}{T}c_{NO2} - \frac{p_0}{T_0}c_{NO2,0}\right), \quad (4)$$

where $\sigma_{PAS,raw}$ is given by Eq. (1) and σ_0 and $c_{NO2,0}$ are $\sigma_{PAS,raw}$ and c_{NO2} during the PAS zero calibration, respectively. Since the zero calibration is performed with particle-free, but not NO_2 denuded air, it is also necessary to include the $c_{NO2,0}$ term which accounts for the NO_2 bias in σ_0. During the dry period of the SMOCC campaign, the period with the largest NO_2 contribution, an average of 6.5% of the PAS signal could be attributed to NO_2. However, since not the absolute NO_2 concentration but the deviation from $c_{NO2,0}$ enters Eq. (4), the NO_2 correction term was typically less than 1% of σ_{PAS}, except for a few instances where sudden drastic changes in pollution levels intermittently enhanced the NO_2 correction term to up to 20%.

In addition to NO_2 interference, the PAS data may be biased by (partial) aerosol volatilization due to laser-induced particle heating, since the latent heat of vaporization would reduce the amount of laser energy generating the acoustic wave and hence reduce the apparent σ_{PAS} (Raspet et al., 2003). For a PAS similar to the one used here, Arnott et al. (2003) showed that for atmospheric aerosol with a deliquescence point of $RH \sim 60\%$ the volatilisation effect was negligible (<10%) up to RH levels of about 80%. Considering the relatively small average hygroscopic diameter growth during SMOCC (<1.04 for RH<45%; Rissler et al., 2005), we anticipate no bias in the PAS signal due to water evaporation. This is corroborated by the absence of a phase shift between PAS microphone signal and oscillating laser power during the SMOCC campaign, which also indicates a negligible PAS bias due to mass transfer effects (Arnott et al., 2003).

Based on these considerations we estimate the accuracy of the PAS under field conditions as better than 10% (95% confidence level) for σ_{PAS}>10 Mm^{-1}, which is larger than the 5% accuracy achieved under controlled laboratory conditions, since it includes the uncertainties due to unavoidable instabilities in operating conditions and NO_2 concentrations. For averaging periods of 5, 15 and 60 min, the instrument noise (precision) was 1.1, 0.7 and 0.4 Mm^{-1}, respectively, which results in a lower detection limit (three times the 1σ noise level) of 1.6, 1.1 and 0.6 Mm^{-1}, respectively.

ACPD
5, 9355–9404, 2005

2.4. Aethalometer

2.4.1. Principle

The 7-λ Aethalometer (AE30, Magee Scientific) measures light attenuation ATN at seven wavelengths (450, 571, 590, 615, 660, 880, and 950 nm, where the 571 nm channel had to be discarded for reasons discussed below) through an aerosol-laden quartz filter based on (Hansen et al., 1984)

$$ATN = 100 \ln\left(\frac{I_0}{I}\right), \tag{5}$$

where I and I_0 are the light intensities transmitted through the particle-laden and a blank spot of the filter, respectively. If aerosol is deposited onto the filter for a time period Δt, the attenuation coefficient σ_{ATN} is given by

$$\sigma_{ATN} = \frac{A}{100Q}\frac{\Delta ATN}{\Delta t}, \tag{6}$$

where A is the area of the aerosol-laden filter spot and Q is the volumetric sampling flow rate. The standard output protocol of the manufacturer provides equivalent black carbon mass concentration BC_{ATN} (g m^{-3}), which is determined from σ_{ATN} according to

$$BC_{ATN} = \frac{\sigma_{ATN}}{\alpha_{ATN}} \tag{7}$$

and

$$\alpha_{ATN}\left[\mathrm{m^2 g^{-1}}\right] = 14\,625/\lambda\,[\mathrm{nm}], \tag{8}$$

where the spectral mass specific attenuation cross-section α_{ATN} is based on the calibration at 880 nm provided by Gundel et al. (1984) utilizing the Malissa-Novakov method, a solvent-based thermal desorption method for elemental carbon analysis.

ACPD
5, 9355–9404, 2005

Since the reliability of thermal desorption methods is still under debate (Schmid et al., 2001), we avoid the resulting uncertainties by limiting our investigation to σ_{ATN}, the primary measurement parameter of the Aethalometer. Hence, each 15 min BC_{ATN} value was converted into σ_{ATN} according to Eqs. (7) and (8).

2.4.2. Relating attenuation and absorption

It is well-known that σ_{ATN} is generally larger than σ_a due to optical interactions of the filter substrate with the deposited aerosol (Petzold et al., 1997; Kopp et al., 1999; Ballach et al., 2001; Weingartner et al., 2003; Arnott et al., 2005). The most significant filter-particle interactions and the resulting biases are: (1) multiple scattering of light at the filter fibers enhances the optical path length and hence imposes a positive bias on σ_{ATN}, (2) enhanced absorption of scattered light with increasing filter loading reduces the optical path length and hence σ_{ATN}, and (3) the filter reflectance (scattering in backwards hemisphere) and hence the measured ATN depends on the optical properties of the deposited particles (bias in σ_{ATN} depends on physico-chemical properties of the particles).

Recently, Arnott et al. (2005) have introduced an Aethalometer calibration equation of the form

$$\sigma^*_{\text{aeth}} = \frac{\sigma_{ATN} - m_s \sigma_s}{C^* \, R\,(ATN)}, \tag{9}$$

where the constant factor C^* ($\geq$1) corrects for multiple light scattering effects within the filter, $R(ATN)$ ($\leq$1) accounts for the 'shadowing' effect due to the filter loading (decrease in Aethalometer sensitivity), and m_s represents the fraction of the aerosol scattering coefficient σ_s that is erroneously interpreted as attenuation. For reasons discussed below, it was not possible to use Eq. (9) for correcting the SMOCC data. Hence, we simplify Eq. (9) to the expression suggested by Weingartner et al. (2003)

$$\sigma_{\text{aeth}} = \frac{\sigma_{ATN}}{C \, R\,(ATN)}, \tag{10}$$

where C^* and the aerosol scattering term are lumped into the new constant C. While Weingartner et al. (2003) introduced this expression under the premise of negligible particle scattering effects, we will show below that its application to the SMOCC data is justified, although particle scattering may not be negligible.

Since the shadowing factor (R) is small for lightly loaded filters (ATN<10) (Weingartner et al., 2003), C can be determined from

$$C = \frac{\sigma_{10}}{\sigma_{\mathrm{PAS}}}, \tag{11}$$

where σ_{10} represents all σ_{ATN} values for ATN<10 (i.e., R≈1) and σ_{PAS} is the PAS-based reference value for absorption. Since the loading correction can be expressed as (Weingartner et al., 2003)

$$R\,(ATN) = \left(\frac{1}{f} - 1\right)\frac{\ln ATN - \ln 10}{\ln 50 - \ln 10} + 1, \tag{12}$$

f can be determined by fitting Eq. (12) to the measured R values given by

$$R_{\mathrm{meas}}\,(ATN) = \frac{\sigma_{ATN}\,(ATN)}{\sigma_{\mathrm{PAS}} C}, \tag{13}$$

where R_{meas} can be interpreted as the loading dependent Aethalometer sensitivity. The difference in wavelength is accounted for by converting one of the Aethalometer channels (σ_{ATN,λ_0}) to the PAS wavelength λ (532 nm) according to

$$\sigma_{ATN} = \sigma_{ATN,\lambda_0}\left(\frac{\lambda}{\lambda_0}\right)^{-a_{ATN}}, \tag{14}$$

where the attenuation Ångström exponent a_{ATN} was calculated from two Aethalometer channels using

$$a_{ATN} = -\frac{\log \sigma_{ATN,0} - \log \sigma_{ATN,1}}{\log \lambda_0 - \log \lambda_1}. \tag{15}$$

ACPD
5, 9355–9404, 2005

2.4.3. Effect of aerosol scattering on attenuation

Finally, we assess the effect of aerosol light scattering on σ_{ATN} and hence on C. According to Eqs. (9) and (10) we can write

$$C^* = \frac{C\,(\sigma_{ATN} - m_s\sigma_s)}{\sigma_{ATN}}. \tag{16}$$

Using the definition of the single scattering albedo

$$\omega_0 = \frac{\sigma_s}{\sigma_s + \sigma_a}, \tag{17}$$

we can substitute σ_s in Eq. (16) by

$$\sigma_s = \frac{\omega_0}{1-\omega_0}\sigma_a, \tag{18}$$

yielding

$$C^* \approx C\left[1 - \frac{m_s\omega_0}{C\,(1-\omega_0)}\right], \tag{19}$$

where the approximation $\sigma_{ATN}/\sigma_{\text{aeth}} \approx C$ was used (i.e., we neglected the loading factor R in Eq. (10), which is relatively close to unity (0.9±0.1 at 532 nm as will be shown below). Equation (19) shows that the aerosol scattering effect (m_s term) increases with ω_0 and decreases with C (multiple scattering from the filter matrix). Furthermore, Eq. (19) implies that, if ω_0 is relatively constant, the aerosol scattering effect becomes a constant correction to the multiple scattering effect (C^*), which is the justification for applying Eq. (10) (instead of Eq. 9) to the SMOCC data as will be discussed below.

2.4.4. Spectral dependence of calibration factors

Since the Aethalometer calibration is performed with a single wavelength PAS, we have to consider the dependence of the correction factors f and C on wavelength. For a

wide variety of soot particles (internally/externally mixed; fresh/aged), Weingartner et al. (2003) showed that the shadowing factor f, while weakly dependent on ω_0, is relatively independent of wavelength. In response to some recent misinterpretations of this finding (e.g. Kirchstetter et al., 2004) we note that this does not mean that the loading correction (R) itself is wavelength independent. R depends on ATN (Eq. 12), which increases with decreasing wavelength. Hence, R (≤1) increases with wavelength, i.e., the loading effect decreases.

Regarding the multiple scattering correction, Weingartner et al. (2003) found only a minor increase of C (<10%) when comparing the 450 and 660 nm channels. A similarly modest dependence of C^* on wavelength (5% increase from 470 to 660 nm) was reported by Arnott et al. (2005). However, since Arnott et al. (2005) also reported a wavelength dependent aerosol scattering correction (m_s) one should consider the overall correction factor C as given by Eq. (19)

$$C = C^* + m_s \frac{\omega_0}{1 - \omega_0}, \tag{20}$$

where the approximation sign was replaced by an equal sign, since the loading correction is irrelevant for this discussion. Using the calibration parameters provided by Arnott et al. (2005), and describing the wavelength dependence of ω_0 by choosing reasonable Ångström exponents for absorption and scattering (a_a and a_s) we can calculate C for wavelengths between 370 and 950 nm.

The results are shown in Table 1 for an assumed ω_0(521 nm)=0.92 (given by Chand et al., 2005, for 545 nm), a_s=2 (Chand et al., 2005) and a_a=1, 1.5, and 2. It is evident that, for an increase in wavelength from 470 to 660 nm, C increases by between 6.5 and 15.4% (depending on a_a), which is comparable to the observations by Weingartner et al. (2003). For the entire spectral range of the AE30 (450 to 950 nm), we might expect a 10, 21 and 36% change in C for a_a=1, 1.5 and 2, respectively, where our data suggest that a_a=1.5 is the most realistic value for the SMOCC data. Hence, we argue that adopting the calibration factors f and C determined at 532 nm for all AE30 channels induces a relatively small error of no more than about 20% (for the most

affected channel at 950 nm).

2.5. PSAP

The Particle Soot Absorption Photometer (PSAP; Radiance Research) described by Bond et al. (1999) measures aerosol light absorption at nominally 565 nm from the light transmitted through an aerosol-laden quartz filter, very similar to the principle of the Aethalometer. Using the difference method as reference Bond et al. (1999) calibrated the PSAP with pure nigrosin and ammonium sulphate particles as well as internal mixtures of both. Analogous to the calibration equation used for the Aethalometer (see Eq. 9) they found

$$\sigma_{\mathrm{PSAP,Bond}} = \frac{\sigma_{\mathrm{raw,PSAP}} K_Q K_A - K_1 \sigma_s}{K_2} = \frac{\sigma_{\mathrm{raw,PSAP}} K_Q K_A}{K_2 + K_1 \frac{\omega_0}{1-\omega_0}}, \quad (21)$$

where $\sigma_{\mathrm{raw,PSAP}}$ is the absorption coefficient reported by the PSAP, K_Q and K_A are the correction factors for flow rate and deposit area, and the calibration constants K_1 and K_2 are given by K_1=0.02±0.02 and K_2=1.22±0.2 (95% confidence level), respectively. Here we used the $\sigma_{\mathrm{raw,PSAP}}$ given on a logarithmic scale and the flow rate was artificially set to a constant internal value of 0.5 L min^{-1}, which did not correspond to the true flow rate, but made it simple to correct for the true flow rate Q by using K_Q=0.5/Q, where Q is given in L min^{-1}. Similarly the true diameter of the deposit spot (4.85 mm) deviated from the internally assumed value of 5.1 mm, which resulted in K_A=(4.81/5.1)^2=0.89. The second expression in Eq. (33.5) was derived by applying Eq. (18) with σ_a=$\sigma_{\mathrm{PSAP,Bond}}$. The fact that K_2 does not depend on ATN implies that the loading correction provided by the manufacturer was confirmed at least up to ATN=35 (which corresponds to a transmittance of 0.7). The Bond correction effectively converts the PSAP wavelength from 565 to 550 nm, since their reference device operated at 550 nm. Although Bond et al. (1999) recommend a minimum PSAP filter transmittance of 0.7 (ATN=35), we found no bias down to 0.5 (ATN=70) and hence included

ACPD
5, 9355–9404, 2005

all data with $ATN<70$. Assuming the uncertainties in K_1 and K_2 are purely random and applying the laws of error propagation to Eq. (21) the accuracy (95% confidence level) of the Bond correction is given by

$$\frac{\Delta\sigma_{\mathrm{PSAP,Bond}}}{\sigma_{\mathrm{PSAP,Bond}}} = \frac{\sqrt{(\Delta K_2)^2 + \left(\Delta K_1 \frac{\omega_0}{1-\omega_0}\right)^2}}{K_2 + K_1 \frac{\omega_0}{1-\omega_0}}. \quad (22)$$

For an average ω_0 of 0.92 (as applicable for the SMOCC data), we can estimate the accuracy of the Bond corrected SMOCC data as 21% using the uncertainties of K_1 and K_2 given above.

3. Intercomparison and field calibration of PSAP and Aethalometer

For the field calibration of the PSAP and Aethalometer with the PAS, we only included PAS data that showed no statistically significant zero drift for three consecutive zero calibrations, which typically occurred over the course of 24 h. This resulted in about 105 and 95 h of calibration data from the dry (17 September to 8 October) and intermediate (9 to 30 October) period, respectively. Since we observed no significant difference in Aethalometer calibration factors determined from either of the two periods, we based the PSAP (and Aethalometer) calibration on the entire 200 h of PAS data. Due to the low pollution levels throughout the wet period of the SMOCC campaign, the wet period is excluded from the PSAP and Aethalometer calibration, but will be discussed separately below.

3.1. PSAP

As a first approximation we applied the Bond correction (Bond et al., 1999) to the PSAP ($\sigma_{\mathrm{PSAP,Bond}}$) using the (dry) scattering coefficients (at 545 nm) determined by

the nephelometer connected to the same inlet as the PSAP. Correlating 5 min averages of $\sigma_{PSAP,Bond}$ and σ_{PAS} we found a slope of 0.76 (R^2=0.813), i.e., the PSAP was on average about 24% too low (data not shown). Accounting for the difference between reference wavelength of the Bond correction and the PAS (532 nm) using a $\lambda^{-1.5}$ dependence reduced the slope to 0.72, which is outside the 95% confidence level of the Bond correction (for purely random errors in K_1 and K_2). On the other hand, our analysis revealed no systematic dependence of $\sigma_{PSAP,Bond}$ on either filter loading or particle single scattering albedo, i.e., the Bond correction adequately accounted for these effects. However, we found a systematic dependence on instrument RH for RH<35%. As seen from Fig. 3a, the ratio of $\sigma_{PSAP,Bond}$ and σ_{PAS} was about constant for 35<RH<55% ($\sigma_{PSAP,Bond}/\sigma_{PAS}$=1.18; or 1.057, if the PAS is corrected to 550 nm), where the data between 45 and 55% are not shown here. On the other hand, for 20%<RH<30%, $\sigma_{PSAP,Bond}/\sigma_{PAS}$ monotonically decreased with RH down to about 0.67 (0.6 for 550 nm). Although Bond et al. (1999) clearly dried their calibration aerosol, the actual RH value was not mentioned. However, we can probably assume that it has been fairly constant under controlled laboratory conditions, i.e., a potential dependence on RH would have introduced a systematic error in K_2. There is some qualitative evidence for an RH sensitivity of the PSAP in the literature. For instance, Arnott et al. (2003) reported an erratic response of the PSAP for rapidly changing RH and Guyon et al. (2004) had to discard PSAP data, if RH exceeded 92%. The observed RH dependence of the PSAP can be numerically described as

$$\sigma_{PSAP,Bond}/\sigma_{PAS} = -0.9212 + 0.1047\,RH - 0.0013\,RH^2 \quad (23)$$

(solid line in Fig. 3a), where RH (given in %) varies between 20 and 45%. The RH corrected PSAP data (σ_{PSAP}) showed excellent correlation (R^2=0.954) and agreement (slope=0.945±0.042) with σ_{PAS} as seen in Fig. 3b, where we neglected PAS values smaller than 4 Mm^{-1} to avoid potentially larger uncertainties near the lower detection limit.

It is noteworthy that during the SMOCC campaign all low RH data were gathered during night due to a higher efficiency of the Nafion drier, and that during night RH

oscillated on a time scale of about 25 min and an amplitude of ∼1.0% (absolute) due to fluctuations in the room temperature (air-conditioner turned periodically on and off). These *RH* oscillations frequently (not always) induced oscillations in $\sigma_{PSAP,Bond}$ that were significantly larger than predicted by Eq. (23). Hence, we eliminated them by applying a running average over one oscillation period. Equation (23) is based on these oscillation corrected data. After removal of these oscillations we did not observe any systematic difference between day and night data that could not be described by the single *RH* correction equation given above. Hence, we estimate the accuracy (95% confidence level) and precision (of 5 min averages) of σ_{PSAP} (532 nm) as about 15% and 12%, respectively.

3.2. Aethalometer

In contrast to the PSAP, the operating conditions of the Aethalometer (AE30) differed from those of the PAS in that the Aethalometer was sampling under ambient conditions (no drier) from a 10 μm inlet (PAS: 1.5 μm impactor). As mentioned above, the average effect of the different cut-off diameters on aerosol absorption has been estimated as less than 6%, and the effect of *RH* will be discussed below. To account for the wavelength dependence of absorption, the 590 nm channel of the Aethalometer was converted to 532 nm according to Eqs. (14) and (15) using λ_1=450, λ_0=590 nm and λ=532 nm. Although the AE30 has an even closer channel at 571 nm, it had to be discarded, since for unknown reasons it was consistently too low by about 20%. The Aethalometer calibration was performed using data with the highest available time resolution (for the Aethalometer: 15 min averages).

3.2.1. Multiple scattering and loading correction

Following Eq. (11) the multiple scattering correction factor C=5.23±0.17 was determined from the arithmetic mean (95% confidence level of the mean) of the ratios of σ_{10} and σ_{PAS} (see Fig. 4), where again we limited σ_{PAS} to values larger than 4 Mm^{-1}.

When recalculating C with the Aethalometer data adjusted for filter loading (see below), C had to be adjusted from its initial value of 5.13 to 5.23. The multiple scattering correction is by far the most important effect when inferring σ_{aeth} from σ_{ATN}.

The effect of filter loading on Aethalometer sensitivity is expressed by Eq. (13). Figure 5 depicts this effect for six consecutive filter cycles (R_{meas}, solid diamonds), where at about ATN=75 (triangles) the filter tape is automatically forwarded to expose a pristine filter spot (ATN~0) to the sample flow. Fitting Eq. (12) to R_{meas} yields f=1.20, where we set R=1 for ATN<10 to be consistent with the assumption adopted for determining C from Eq. (11). Obviously, the shadowing effect accounts for a maximum sensitivity reduction of about 20% (at 532 nm). As shown in Fig. 5 (dashed line) using the more rigorously derived form of the loading correction presented by Arnott et al. (2005) yields a very similar result. The poor correlation coefficient between data and fit (R^2~0.5) is a result of the relatively small effect of filter loading (<20% at 532 nm) compared to the multiple scattering correction factor of 5.23. Hence, small fluctuations in C may obfuscate the filter loading effect. As discussed below possible culprits for such fluctuations are instrument RH, ω_0, and gaseous adsorption.

3.2.2. Dependence on sampling period

Since the Aethalometer response is known to depend on aerosol properties and hence on sampling location (Petzold et al., 1997; Arnott et al., 2005), it is conceivable that the correction factors C and f varied with pollution level and sampling period. Using C=5.23 and f=1.20, Figs. 6a and b show the ratio of σ_{aeth} and σ_{PAS} as a function of the pollution level (indicated by σ_{PAS}) for both the dry and transition period of the SMOCC campaign, respectively, where the seasonal mean values of 0.943 and 1.034, respectively, are indicated by horizontal lines. While there is no systematic dependence of $\sigma_{\text{aeth}}/\sigma_{\text{PAS}}$ on σ_{PAS} for the transition period, there is a small negative trend for the dry period, which will result in a 13% difference in slopes derived from the linear regression of a scatter plot of σ_{aeth} and σ_{PAS} (data not shown) given by σ_{aeth}=0.87 σ_{PAS} (Mm^{-1})+0.98 Mm^{-1} (R^2=0.91) and σ_{aeth}=1.00 σ_{PAS} (Mm^{-1})+0.49 Mm^{-1} (R^2=0.73) for

the dry and intermediate period, respectively. This enhancement of σ_{aeth} for the transition period is consistent with the previously discussed enhanced aerosol mass bias induced by the difference in inlet cut-off diameters (10 μm versus 1.5 μm). However, despite these small differences we conclude that there is no systematically significant dependence of the Aethalometer correction factors on sampling period. Thus, unless stated otherwise, we will henceforth not distinguish between dry and transition period.

For the wet season, it was impossible to calibrate the Aethalometer and PSAP, mainly due to the poor signal-to-noise ratio and the unavoidable small drifts in zero offset of the PAS. Hence, for lack of a better alternative, we recommend to apply the correction factors derived for the dry and transition period also to the Aethalometer and PSAP data of the wet period.

3.2.3. Dependence on relative humidity

As mentioned above, while the PAS was operated under dry conditions (RH<45%), the sample air supplied to the Aethalometer was not actively dried, i.e., it closely approximated ambient conditions. Figure 7 depicts the Aethalometer-based ambient absorption coefficient (σ_{aeth}) normalized to dry absorption (σ_{PAS}) as a function of RH. For each RH segment, the mean and 95% confidence level of the mean was calculated. It is evident that there is no statistically significant dependence of σ_{aeth} on RH at least between 40 and 80% RH.

3.2.4. Dependence on single scattering albedo ω_0

The effect of ω_0 on the Aethalometer signal can be assessed based on Eq. (19). Laboratory studies by Weingartner et al. (2003) and Arnott et al. (2005) reported m_s values of 0.008 and 0.055 (at 550 nm), respectively, for purely scattering aerosol (i.e., up to 5.5% of aerosol light scattering is erroneously interpreted as attenuation). During the dry and transition period of the SMOCC campaign, ω_0 was relatively constant at 0.92±0.02 (Chand et al., 2005). Using Eq. (19) with m_s=0.055 as an estimated up-

per limit of the aerosol scattering effect, we can attribute 13.0±3.5% of the observed multiple scattering correction C (=5.23) to aerosol light scattering, i.e., the multiple scattering factor corrected for aerosol scattering is given by C^*=4.55. Furthermore, since the small variability in ω_0 (±0.02) translates into a relatively small effect (3.5%) on C, it was impossible to distinguish the aerosol scattering (m_s) from the multiple scattering effect of the filter substrate, i.e., we had to rely on Eq. (10) instead of on Eq. (9) for the Aethalometer calibration.

3.2.5. Gaseous adsorption onto the filter

Gaseous adsorption onto quartz filters is a well-known phenomenon that potentially enhances the multiple scattering effect of the filter, and hence introduces a positive bias in C (Kirchstetter et al., 2001). The intuitive approach for an investigation of this effect is to look for systematically enhanced C values for large pollution levels. However, since each Aethalometer measurement cycle begins with an acclimatization phase, which exposes the (initially) clean filter spot to ambient air without taking data, and references the measured attenuation to the zero value obtained during this acclimatization phase, a potential dependence of C on pollution level is eliminated. This explains why we found no statistically significant dependence of C on sampling period despite the substantially higher pollution levels during the dry period (average σ_a (550 nm) = 22.9 and 7.5 Mm^{-1} for the dry and intermediate season, respectively). However, if gaseous adsorption introduces a bias into C it can be detected according to the following rationale. Let us assume that at time point t_0 the filter is in equilibrium with the gas phase, i.e., there is no net transport of gas molecules to or from the filter. If the pollution level changes at time point t_1, there will be a net transport of gas molecules to or from the filter depending on whether the pollution level increases or decreases. If the relaxation time for this process is larger than the averaging time of the Aethalometer (here 15 min) one would expect a systematic bias in C with the gradient in pollution level. We investigated this effect by comparing the relative change in C and σ_{aeth}, where σ_{aeth} is a proxy for the pollution level. For two time layers i and i + 1, the temporal gradients of the pollution

level and C can be expressed as

$$\frac{\Delta\sigma_{\text{aeth}}}{\sigma_{\text{aeth}}} = \frac{\sigma_{\text{aeth}}^{i+1} - \sigma_{\text{aeth}}^{i}}{\left(\sigma_{\text{aeth}}^{i+1} + \sigma_{\text{aeth}}^{i}\right)/2} \tag{24}$$

and

$$\frac{\Delta C}{C} = \frac{C^{i+1} - C^{i}}{\left(C^{i+1} + C^{i}\right)/2}, \tag{25}$$

respectively. As seen from Fig. 8, there is a positive correlation (R^2=0.45) between the change in pollution level and C, which is consistent with the hypothesis that adsorption of gaseous components will enhance the multiple scattering of the filter matrix. This analysis indicates that about 45% of the previously unexplained variability in the Aethalometer signal can be attributed to gaseous adsorption and, at least for σ_{aeth} gradients up to 20% per 15 min, we find

$$\Delta C/C = (0.854 \pm 0.028)\,\Delta\sigma_{\text{aeth}}/\sigma_{\text{aeth}}\,. \tag{26}$$

It is noteworthy that this equation holds for both the dry and the transition period, i.e., it is independent of the absolute value of σ_{aeth}. On the other hand, no adsorption effect at all was found for the PSAP (R^2=0.04).

3.2.6. Accuracy

We estimate the accuracy (95% confidence level) and precision (for 15 min averages) of the corrected Aethalometer data as about 20% and 35%, respectively (except for the 571 nm channel, which was systematically too low), at least in the vicinity of the calibration wavelength (450–600 nm). Although assumed constant here, slightly larger values of C are expected for larger wavelengths, as discussed in Sect. 2.4.4 (cf. Table 1). Thus, the quoted accuracy is lower than for the PSAP to account for additional uncertainties due to wavelength conversion (uncertainties in a_a) and the use of different inlets.

4. Discussion

It is instructive to compare our findings with previous studies. The PSAP was used in numerous field studies (Reid et al., 1998; Mader et al., 2002; Wex et al., 2002; Arnott et al., 2003; Guyon et al., 2003a, b). Since the laboratory calibration factors by Bond et al. (1999) became available, the ambient PSAP data were corrected for instrument artifacts. Recently, the laboratory study by Virkkula et al. (2005a) has essentially confirmed the Bond correction for external mixtures of kerosene soot and ammonium sulphate particles. However, the observed deviations for pure soot (from a kerosene lamp) and purely scattering particles resulted in the derivation of a new (ω_0 dependent) loading correction. Keeping in mind that the Bond calibration was performed with spherically shaped particles (internal mixtures of nigrosin and ammonium sulphate), inconsistencies for fractal-like soot particles may not be too surprising. Unfortunately, Virrkula et al. (2005a) was unable to derive a 'unified' correction scheme that would be applicable to all types of aerosols used (ammonium sulphate, PSL, soot, and external mixtures thereof). However, they noted that for their ~1.5 day outdoor experiment in Reno, NV, the two correction schemes resulted in less than 6% difference. The difference compared to the reference method was within 20%, and part of this deviation was probably due to sensitivity limits of the PAS that was used as reference method. To our knowledge, there are only two more field calibrations with a true in-situ reference method such as the difference method or the PAS. The study by Reid et al. (1998) did not account for PSAP artifacts, since it was performed prior to Bond et al. (1999) and Arnott et al. (2003) found that σ_{PSAP} was by a factor of 1.61 larger than σ_{PAS} for rural aerosols from the North Central Oklahoma. Combined with the good accuracy of the Bond correction for pyrogenically affected aerosols from the Amazon Basin as reported in this study, we conclude that the Bond correction is quite adequate for most ambient aerosols with two possible exceptions: (1) purely fractal-like and scattering (i.e., ω_0 close to unity) particles and (2) varying and/or low RH conditions (RH<30%). However, we add as caveat, that the dependence on RH should be confirmed under

ACPD
5, 9355–9404, 2005

controlled laboratory conditions. Both Guyon et al. (2003b) and this study found that (at least for Amazonian aerosol) the Bond correction could be extended beyond the original transmittance limit of 0.7 down to 0.5, which corresponds to $ATN<70$. It is also noteworthy that, in contrast to the Aethalometer, there is no correlation between $\Delta C/C$ and $\Delta\sigma_{aeth}/\sigma_{aeth}$ for the PSAP (R^2=0.04), i.e., gaseous adsorption does not seem to affect the PSAP performance. We attribute this to the different types of filter used.

Previous Aethalometer calibrations with laboratory-generated aerosols mostly reported multiple scattering factors (C) close to 2. As mentioned above, while Arnott et al. (2005) found C values between 1.8 and 2.2 (depending on wavelength) in the laboratory, they reported C=3.7 (at 521 nm) for ambient (urban) aerosols, where strictly speaking Arnott et al. (2005) referred to C^* , i.e., C corrected for aerosol scattering effects, which was found to be 4.55 for the SMOCC data. Similarly, the laboratory study by Weingartner et al. (2003) found C=2.14 for both pure soot (Diesel and PALAS) and external soot mixtures (with ammonium sulphate). On the other hand, for soot (Diesel and PALAS) particles coated with organic carbon (internally mixed aerosol) their C value increased to 3.6. Clearly our value of C=5.23 (or 4.55, if compared to Arnott et al., 2005) compares more favourably with the ambient or internal mixture measurements performed by Arnott et al. (2005) and Weingartner et al. (2003), respectively. Both Arnott et al. (2005) and Weingartner et al. (2003) offered possible explanations for the factor of ~2 difference in C values. Arnott et al. (2005) hypothesized that variable particle preloading of the filter during the automatically performed filter acclimatization phase prior to any measurement might be responsible for the enhanced C value under ambient conditions. However, in light of a maximum loading correction of no more than 30% (~550 nm), as was consistently reported by Weingartner et al. (2003), Arnott et al. (2005) and the present study, a more than 80% enhancement in C seems hard to justify. On the other hand, Weingartner et al. (2003) speculated that adsorption of semi-volatile organic gaseous components (from the oxidation of α-pinene) onto the filter matrix might have artificially enhanced the multiple scattering within the filter matrix. As mentioned above, since most of this effect should be eliminated by the filter

acclimatization phase and since their experiments were performed for fairly constant source concentrations, we do not consider this a probable explanation either.

Although we are unable to resolve this issue conclusively, we offer a different explanation for the observed difference in C. The significance of the degree and kind of aerosol mixing on light absorption is well known from Mie theory for coated particles (Bohren and Huffman, 1983). For attenuation measurements, Petzold et al. (1997) argued that internally mixed aerosol may enhance the Aethalometer response by up to about a factor of 2 compared to external mixtures for black carbon (BC) mass fractions larger than about 3% (as was the case for the laboratory calibrations by Arnott et al., 2005). Hence, the observed multiple scattering correction factors of 3.7, 3.6 and 4.55 (or 5.23, if the aerosol scattering effect is absorbed into the multiple scattering factor) for urban aerosol (Arnott et al., 2005), organically coated soot particles (Weingartner et al., 2003), and Amazonian aerosols (this study), respectively, may possibly be a result of attenuation enhancement due to internal mixing. This notion is corroborated by the fact that the Bond correction of the PSAP, which as discussed above demonstrates good applicability to ambient aerosol, was performed with internal mixtures of nigrosin and ammonium sulphate (Bond et al., 1999).

The filter loading correction factor R depends on attenuation and hence on λ. At the highest loading prior to the automatic filter change (ATN=75 at 590 nm) R is 0.76, 0.8 and 0.85 for λ=450, 532, and 950 nm, respectively, i.e., the measured attenuation coefficient on a pristine filter is 32, 25, and 18% larger than a fully loaded filter, respectively. This is consistent with the values reported by Weingarter et al. (2003) who also showed that the loading correction factor f is related to ω_0 by $f=A\ (1\text{-}\omega_0)+1$, where A=0.86±0.1. Using f=1.2, as derived above, this yields ω_0=0.77±0.03, which is not consistent with the observed ω_0 of about 0.92. However, Weingartner et al. (2003) acknowledged that the reliability of A is limited due to the relatively large scatter in their data. In addition, most of their data was acquired for ω_0<0.6 and the few data points with ω_0>0.6 have large error margins. Hence the apparent inconsistency between f and ω_0 is not surprising especially, if we also consider that R not only depends on ω_0

but on how deep the aerosol is embedded into the filter matrix (Arnott et al., 2005), which may depend on particle size and morphology as well as on sampling flow rate.

As seen from our PSAP calibration, RH may affect the response of filter-based absorption measurements. In addition, hygroscopic aerosol growth may 'truly' enhance aerosol light absorption due to the optical interaction between aerosol core and coating (Fuller et al., 1999). However, Fig. 7 shows no dependence of σ_{aeth} on RH within the experimental uncertainty at least for RH between 40 and 80%. This is consistent with the relatively small hygroscopic diameter growth factor of <1.1 at RH=80% as reported by Rissler et al. (2005) for collocated hygroscopic growth measurements.

The relatively large scatter in Aethalometer data, which results in a rather poor precision of 35%, is an important aspect. We attribute this in part to gaseous adsorption onto the filter as depicted Fig. 8. This becomes evident when we consider the mean (two standard deviations about the mean) of the normalized σ_{aeth} for, e.g., the dry period. When we apply the adsorption correction according to Eq. (26), we find $\sigma_{aeth}/\sigma_{PAS}$=0.947±0.26 for the dry period. Comparing this to the uncorrected values of 0.943±0.36 (see Fig. 6a), we see that precision has improved from 35% to 26%, while the average value has not changed as is to be expected, since over long periods of time the positive and negative gradients in pollution level should add up to zero. Hence, implementing the adsorption correction will enhance the precision, but not the accuracy of the Aethalometer. As mentioned above, the effect of gaseous adsorption on instrument accuracy should be relatively well accounted for by allowing for filter acclimatization (i.e., exposing the filter to ambient air) prior to the first measurement.

There are substantial differences in the response of the PSAP and Aethalometer to changes in RH. While the normalized PSAP response increased by a factor of 2 for an increase in RH from 20 to 30% (Fig. 3a), no statistically significant dependence on RH was found for the Aethalometer (Fig. 7). Keeping in mind that the PSAP and PAS were operated at the same (but varying) RH level, the observed dependence of $\sigma_{PSAP,Bond}/\sigma_{PAS}$ on RH has to be an instrument artifact of either the PSAP or the PAS. As mentioned above, there is both theoretical and experimental evidence for the ab-

ACPD
5, 9355–9404, 2005

sence of an RH effect on the PAS for RH<80% (Raspet et al., 2003; Arnott et al., 2003). Hence, we attribute the observed RH dependence of $\sigma_{PSAP,Bond}/\sigma_{PAS}$ to a systematic error of the PSAP, possibly related to a wettability threshold of the PSAP filter near RH=25%. As mentioned above, in contrast to the PAS (and the PSAP), the air flowing into the Aethalometer was not actively dried, i.e. the RH in the Aethalometer was always larger than the RH in the PAS. Hence, Fig. 7 depicts the combined effect of particle hygroscopicity and potential instrument artifacts. Analogous to our discussion of gaseous adsorption, RH related Aethalometer artifacts should be at least partially accounted for by the filter acclimatization phase. Thus, one might conclude from Fig. 7 that there is no hygroscopic absorption enhancement. This is consistent with the theoretical predictions of Redemann et al. (2001), who found an hygroscopic enhancement factor at λ=550 nm for sulphuric acid coated soot particles with a realistic lognormal size distribution (geometric mean diameter and standard deviation of 0.12 μm and 1.5, respectively) of about 1.1 at RH=80%. Considering the relatively small hygroscopic diameter growth factor of less than 1.08 (RH=80%) for Amazonian aerosols (Rissler et al., 2005), we consider this growth factor to be an upper limit for our study. However, we add as an important caveat that the Aethalometer may not be capable at all of accurately measuring the electromagnetic focusing effect of absorbing particles enclosed by a liquid coating, since the shape (and hence the optical properties) of the partially liquid particle is expected to change upon deposition onto a filter substrate.

Finally, in Figs. 9a and b we compare 1 h averages of PSAP and Aethalometer (adjusted to 532 nm based on a power-law fit of the measured spectral absorption) data for the dry and transition period, respectively. It is evident that the instruments are well correlated for both periods (dry: R^2=0.88; transition: R^2=0.90) and, forcing the linear regression line through the origin, it is evident that σ_{PSAP} is by about 9.8% larger (slope = 1.098±0.047) and 2.5 % smaller (slope = 0.975±0.030) than σ_{aeth} for the dry and transition period, respectively. Considering that Fig. 9 represents more than 2 months of data, while the calibration of the PAS and PSAP was based on only 200 h, the agreement of the instruments is quite satisfactory and the slopes agree within the

estimated instrument accuracies. On the other hand, the correlation is weaker for σ_a>40 Mm^{-1}, which we attribute to the scarcity of PAS data for this absorption range as seen from Figs. 3 and 6. Hence, we add as a caveat that the reliability of the PSAP and Aethalometer calibration is somewhat weaker for σ_a>40 Mm^{-1}, although even in this range the agreement between PSAP and Aethalometer is better than 25%, the estimated 2σ level based on the instrument accuracies.

5. Conclusions

A 1-λ PSAP (Particle Soot Absorption Photometer, 565 nm) and a 7-λ AE30 Aethalometer were compared against a PAS (photoacoustic spectrometer, 532 nm) based on 200 h of collocated ambient sampling at a rural site in the Amazon Basin during the dry and wet-dry transition period of the LBA-SMOCC campaign in 2002. To ensure data quality we verified the PAS accuracy of 10% in the field following the calibration procedure described by Arnott et al. (2000) using NO_2 as calibration gas.

The calibration of the PSAP with the PAS essentially confirmed the Bond correction (Bond et al., 1999), except for a not previously reported sensitivity decrease for low *RH* values (20 to 30%). On the other hand, we found a significantly larger multiple scattering correction factor of C=5.23 than determined by previous calibrations (C~2). Although the effect of aerosol scattering was indistinguishable from multiple scattering effects, we estimated the contribution of aerosol scattering to C to be no more than 13% (=1–4.55/5.23). Since our C value is relatively consistent with the few available measurements for internally mixed laboratory and ambient aerosols, we propose that this difference is at least in part due to differences in the mixing state of the aerosol, i.e., internally mixed (ambient) aerosols has elevated mass attenuation cross sections. For black carbon mass fractions larger than 3%, this hypothesis is supported by the theoretical calculations of Petzold et al. (1997).

The wavelength-dependent loading correction was considerably smaller than the multiple scattering correction, and it decreased for the Aethalometer from a maximum

ACPD
5, 9355–9404, 2005

of 32 to 18% for λ increasing from 450 to 950 nm. For the PSAP, the manufacturer-provided loading correction was found to be adequate for transmission down to 0.5 (ATN<70). Based on the limited available information in the literature, we argue that the Aethalometer correction factors (C=5.23 and f=1.20), which were determined at 532 nm, are approximately independent of λ, i.e., they can be applied to all Aethalometer channels. For unknown reasons, the 571 nm channel of the Aethalometer was consistently by about 20% too low.

In addition, a potential sensitivity of the PSAP and Aethalometer to RH was investigated. While the Aethalometer showed no sensitivity to gradual RH changes between 40 and 80%, the PSAP displayed a positive quadratic dependence to RH for 20%<RH<30%. This finding may in part have been due to inadvertent oscillations in room temperature (and hence in RH) during nighttime sampling. However, no such dependence was found for RH values between 30 and 55%. While the absence of an hygroscopic absorption enhancement for an increase in RH from about 40 to 80% is consistent with theoretical predictions (Redemann et al., 2001), it is questionable whether humidified particles deposited onto a filter substrate display the same optical properties as in the suspended state.

Assuming that the PSAP and Aethalometer sensitivity to gaseous adsorption onto the quartz filter matrix should be correlated to temporal gradients in pollution level (here represented by σ_a), we investigated the correlation between instrument response and gradients in σ_a. While we found no such correlation for the PSAP, there was a clear positive correlation for the Aethalometer, leading to a reduction in instrument precision (36% instead of 26%). However, since there was no measurable effect on Aethalometer accuracy, we conclude that the routinely performed filter acclimatization prior to utilizing a new filter adequately accounts for filter adsorption effects. To our knowledge, there has been no previous study of this phenomenon for either the PSAP or the Aethalometer.

This study shows that, while laboratory calibration experiments are useful, on-site calibrations of the PSAP and Aethalometer are required for ambient measurements

to ensure data quality. Although both PSAP and Aethalometer are based on the integrating-plate method, the conversion of the measured attenuation (σ_{ATN}) into absorption (σ_a) requires different correction parameters, which is likely due to the different filter types used. If an on-site calibration cannot be provided, we offer the following suggestions for operating a PSAP or Aethalometer with ambient aerosols: For the PSAP, the Bond correction (Eq. 21) can be applied with an expected uncertainty of at least 20% provided RH is kept constant between about 35 and 55%, although operation up to 90% may also be possible. For the Aethalometer, we suggest a multiple scattering correction factor of 4.2±0.84 (arithmetic mean of 3.6, 3.7 and 5.2; estimated 2σ-accuracy of Aethalometer) and the use of the loading correction as given by Eq. (12) with f=1.2. This should provide an accuracy of about 25%. Additional field calibrations are desirable to confirm these recommendations.

Acknowledgements. This work was carried out within the frame work of the Smoke, Aerosols, Clouds, Rainfall, and Climate (SMOCC) project, a European contribution to the Large-Scale Biosphere-Atmosphere Experiment in Amazonia (LBA). It was financially supported by the Environmental and Climate Program of the European Commission (contract N° EVK2-CT-2001-00110 SMOCC), the Max Planck Society (MPG), the Fundação de Amparo à Pesquisa do Estado de São Paulo, and the Conselho Nacional de Desenvolvimento Científico (Instituto do Milênio LBA). We thank all members of the LBA-SMOCC and LBA-RACCI Science Teams for their support during the field campaign, especially A. C. Ribeiro, M. A. L. Moura, and J. von Jouanne as well as P. Guyon for providing his Mie code and adapting it to our needs.

References

Ackerman, A. S., Toon, O. B., Stevens, D. E., Heymsfield, A. J., Ramanathan, V., and Welton, E. J.: Reduction of tropical cloudiness by soot, Science, 288, 1042–1047, 2000.

Andreae, M. O., Artaxo, P., Brandão, C., Carswell, F. E., Ciccioli, P., da Costa, A. L., Culf, A. D., Esteves, J. L., Gash, J. H. C., Grace, J., Kabat, P., Lelieveld, J., Malhi, Y., Manzi, A. O., Meixner, F. X., Nobre, A. D., Nobre, C., Ruivo, M. d. L. P., Silva-Dias, M. A., Stefani, P., Valentini, R., von Jouanne, J., and Waterloo, M. J.: Biogeochemical cycling of carbon,

water, energy, trace gases and aerosols in Amazonia: The LBA-EUSTACH experiments, J. Geophys. Res., 107, 8066, doi:10.1029/2001JD000524, 2002.

Andreae, M. O., Rosenfeld, D., Artaxo, P., Costa, A. A., Frank, G. P., Longo, K. M., and Silva-Dias, M. A. F.: Smoking rain clouds over the Amazon, Science, 303, 1337–1342, 2004.

Arnott, W. P., Hamasha, K., Moosmüller, H., Sheridan, P. J., and Ogren, J. A.: Towards aerosol light-absorption measurements with a 7-wavelength aethalometer: Evaluation with a photoacoustic instrument and 3-wavelength nephelometer, Aerosol Sci. Technol., 39, 17–29, 2005.

Arnott, W. P., Moosmüller, H., Rogers, C. F., Jin, T., and Bruch, R.: Photoacoustic spectrometer for measuring light absorption by aerosol: Instrument description, Atmos. Environ., 33, 2845–2852, 1999.

Arnott, W. P., Moosmüller, H., Sheridan, P. J., Ogren, J. A., Raspet, R., Slaton, W. V., Hand, J. L., Kreidenweis, S. M., and Collett, J. L.: Photoacoustic and filter-based ambient aerosol light absorption measurements: Instrument comparisons and the role of relative humidity, J. Geophys. Res., 108, 4034, doi:10.1029/2002JD002165, 2003.

Arnott, W. P., Moosmüller, H., and Walker, J. W.: Nitrogen dioxide and kerosene-flame soot calibration of photoacoustic instruments for measurement of light absorption by aerosols, Rev. Sci. Instrum., 71, 4545–4552, 2000.

Ballach, J., Hitzenberger, R., Schultz, E., and Jaeschke, W.: Development of an improved optical transmission technique for black carbon (BC) analysis, Atmos. Environ., 35, 2089–2100, 2001.

Bohren, C. F. and Huffman, D. R.: Absorption and scattering of light by small particles, Wiley, New York, USA, 1983.

Bond, T. C., Anderson, T. L., and Campbell, D.: Calibration and intercomparison of filter-based measurements of visible light absorption by aerosols, Aerosol Sci. Technol., 30, 582–600, 1999.

Chand, D., Guyon, P., Artaxo, P., Schmid, O., Frank, G. P., Rizzo, L. V., Mayol-Bracero, O. L., Gatti, L. V., and Andreae, M. O.: Optical and physical properties of aerosols in the boundary layer and free troposphere over the Amazon Basin during the biomass burning season, Atmos. Chem. Phys. Discuss., 5, 4373–4406, 2005, SRef-ID: 1680-7375/acpd/2005-5-4373.

Fuller, K. A., Malm, W. C., and Kreidenweis, S. M.: Effects of mixing on extinction by carbonaceous particles, J. Geophys. Res., 104, 15 941–15 954, 1999.

Gundel, L. A., Dod, R. L., Rosen, H., and Novakov, T.: The relationship between optical attenuation and black carbon concentration for ambient and source particles, Sci. Total Environ., 36, 197–202, 1984.
Guyon, P., Boucher, O., Graham, B., Beck, J., Mayol-Bracero, O. L., Roberts, G. C., Maenhaut, W., Artaxo, P., and Andreae, M. O.: Refractive index of aerosol particles over the Amazon tropical forest during LBA-EUSTACH 1999, J. Aerosol Sci., 34, 883–907, 2003a.
Guyon, P., Graham, B., Beck, J., Boucher, O., Gerasopoulos, E., Mayol-Bracero, O. L., Roberts, G. C., Artaxo, P., and Andreae, M. O.: Physical properties and concentration of aerosol particles over the Amazon tropical forest during background and biomass burning conditions, Atmos. Chem. Phys., 3, 951–967, 2003b, SRef-ID: 1680-7324/acp/2003-3-951.
Guyon, P., Graham, B., Roberts, G. C., Mayol-Bracero, O. L., Maenhaut, W., Artaxo, P., and Andreae, M. O.: Sources of optically active aerosol particles over the Amazon forest, Atmos. Environ., 38, 1039–1051, 2004.
Hansen, A. D. A., Rosen, H., and Novakov, T.: The aethalometer – an instrument for the real-time measurement of optical absorption by aerosol particles, Sci. Total Environ., 36, 191–196, 1984.
Heintzenberg, J. and Charlson, R. J.: Design and applications of the integrating nephelometer: A review, American Meteorological Society, 13, 987–1000, 1996.
Horvath, H.: Atmospheric light-absorption – a review, Atmos. Environ. Part a-General Topics, 27, 293–317, 1993.
Kirchstetter, T. W., Corrigan, C. E., and Novakov, T.: Laboratory and field investigation of the adsorption of gaseous organic compounds onto quartz filters, Atmos. Environ., 35, 1663–1671, 2001.
Kirchstetter, T. W., Novakov, T., and Hobbs, P. V.: Evidence that the spectral dependence of light absorption by aerosols is affected by organic carbon, J. Geophys. Res., 109, doi:10.1029/2004JD004999, 2004.
Kirkman, G. A., Gut, A., Ammann, C., Gatti, L. V., Cordova, A. M., Moura, M. A. L., Andreae, M. O., and Meixner, F. X.: Surface exchange of nitric oxide, nitrogen dioxide, and ozone at a cattle pasture in Rondonia, Brazil, J. Geophys. Res., 107, 8083, doi:10.1029/2001JD000523, 2002.
Kopp, C., Petzold, A., and Niessner, R.: Investigation of the specific attenuation cross-section of aerosols deposited on fiber filters with a polar photometer to determine black carbon, J.

Aerosol Sci., 30, 1153–1163, 1999.
Liousse, C., Cachier, H., and Jennings, S. G.: Optical and thermal measurements of black carbon aerosol content in different environments: Variation of the specific attenuation cross-section, sigma (s), Atmos. Environ., 27A, 1203–1211, 1993.
Mader, B. T., Flagan, R. C., and Seinfeld, J. H.: Airborne measurements of atmospheric carbonaceous aerosols during ACE-Asia, J. Geophys. Res., 23, 4704, doi:10.1029/2002JD002221, 2002.
Marple, V. A., Rubow, K. L., and Behm, S. M.: A Microorifice Uniform Deposit Impactor (Moudi) – Description, Calibration, and Use, Aerosol Sci. Technol., 14, 434–446, 1991.
McMurry, P. H.: A review of atmospheric aerosol measurements, Atmos. Environ., 34, 1959–1999, 2000.
Moosmüller, H., Arnott, W. P., Rogers, C. F., Chow, J. C., Frazier, C. A., Sherman, L. E., and Dietrich, D. L.: Photoacoustic and filter measurements related to aerosol light absorption during the Northern Front Range Air Quality Study (Colorado 1996/1997), J. Geophys. Res., 103, 28 149–28 157, 1998.
Penner, J. E., Andreae, M. O., Annegarn, H., Barrie, L., Feichter, J., Hegg, D., Jayaraman, A., Leaitch, R., Murphy, D., Nganga, J., and Pitari, G.: Aerosols, their Direct and Indirect Effects, in: Climate Change 2001: The Scientific Basis, Contribution of Working Group I to the Third Assessment Report of the Intergovernmental Panel on Climate Change, edited by: Houghton, J. T., Ding, Y., Griggs, D. J., Noguer, M., van der Linden, P. J., Dai, X., Maskell, K., and Johnson, C. A., pp. 289–348, Cambridge University Press, Cambridge, UK, and New York, NY, USA, 2001.
Petzold, A., Kopp, C., and Niessner, R.: The dependence of the specific attenuation cross section on black carbon mass fraction and particle size, Atmos. Environ., 31, 661–672, 1997.
Petzold, A., Schloesser, H., Sheridan, P. J., Arnott, W. P., Ogren, J. A., and Virkkula, A.: Evaluation of multiangle absorption photometry for measuring aerosol light absorption, Aerosol Sci. Technol., 39, 40–51, 2005.
Petzold, A. and Schönlinner, M.: Multi-angle absorption photometry – a new method for the measurement of aerosol light absorption and atmospheric black carbon, J. Aerosol Sci., 35, 421–441, 2004.
Raspet, R., Slaton, W. V., Arnott, W. P., and Moosmüller, H.: Evaporation-condensation effects on resonant photoacoustics of volatile aerosols, J. Atmos. Ocean Technol., 20, 685–695, 2003.

Redemann, J., Russell, P. B., and Hamill, P.: Dependence of aerosol light absorption and single-scattering albedo on ambient relative humidity for sulfate aerosols with black carbon cores, J. Geophys. Res., 106, 27 485–27 495, 2001.

Reid, J. S., Hobbs, P. V., Liousse, C., Martins, J. V., Weiss, R. E., and Eck, T. F.: Comparisons of techniques for measuring shortwave absorption and black carbon content of aerosols from biomass burning in Brazil, J. Geophys. Res., 103, 32 031–32 040, 1998.

Rissler, J., Vestin, A., Swietlicki, E., Fisch, G., Zhou, J., Artaxo, P., and Andreae, M. O.: Size distribution and hygroscopic properties of aerosol particles from dry-season biomass burning in Amazonia, Atmos. Chem. Phys. Discuss., in press, 2005.

Rosencwaig, A.: Photoacoustics and photoacoustic spectroscopy, Wiley, New York, 1980.

Saathoff, H., Moehler, O., Schurath, U., Kamm, S., Dippel, B., and Mihelcic, D.: The AIDA soot aerosol characterisation campaign 1999, J. Aerosol Sci., 34, 1277–1296, 2003.

Schmid, H., Laskus, L., Abraham, H. J., Baltensperger, U., Lavanchy, V., Bizjak, M., Burba, P., Cachier, H., Crow, D., Chow, J., Gnauk, T., Even, A., ten Brink, H. M., Giesen, K. P., Hitzenberger, R., Hueglin, E., Maenhaut, W., Pio, C., Carvalho, A., Putaud, J. P., Toom-Sauntry, D., and Puxbaum, H.: Results of the "carbon conference" international aerosol carbon round robin test stage I, Atmos. Environ., 35, 2111–2121, 2001.

Schnaiter, M., Schmid, O., Petzold, A., Fritzsche, L., Klein, K.-F., Andreae, M. O., Helas, G., Thielmann, A., Gimmler, M., Möhler, O., Linke, C., and Schurath, U.: Measurement of wavelength-resolved light absorption by aerosols utilizing a UV-VIS extinction cell, Aerosol Sci. Technol., 39, 249–260, 2005.

Sheridan, P. J., Arnott, W. P., Ogren, J. A., Andrews, E., Atkinson, D. B., Covert, D. S., Moosmüller, H., Petzold, A., Schmid, B., Strawa, A. W., Varma, R., and Virkkula, A.: The Reno aerosol optics study: An evaluation of aerosol absorption measurement methods, Aerosol Sci. Technol., 39, 1–16, 2005.

Terhune, R. W. and Anderson, J. E.: Spectrophone measurements of the absorption of visible light by aerosols in the atmosphere, Opt. Lett., 1, 70–72, 1977.

Truex, T. J. and Anderson, J. E.: Mass monitoring of carbonaceous aerosols with a spectrophone, Atmos. Environ., 13, 507–509, 1979.

Virkkula, A., Ahlquist, N. C., Covert, D. S., Arnott, W. P., Sheridan, P. J., Quinn, P. K., and Coffman, D. J.: Modification, calibration and a field test of an instrument for measuring light absorption by particles, Aerosol Sci. Technol., 39, 68–83, 2005a.

Virkkula, A., Ahlquist, N. C., Covert, D. S., Sheridan, P. J., Arnott, W. P., and Ogren, J. A.: A

three-wavelength optical extinction cell for measuring aerosol light extinction and its application to determining light absorption coefficient, Aerosol Sci. Technol., 39, 52–67, 2005b.

Weingartner, E., Saathoff, H., Schnaiter, M., Streit, N., Bitnar, B., and Baltensperger, U.: Absorption of light by soot particles: determination of the absorption coefficient by means of aethalometers, J. Aerosol Sci., 34, 1445–1463, 2003.

Wex, H., Neususs, C., Wendisch, M., Stratmann, F., Koziar, C., Keil, A., Wiedensohler, A., and Ebert, M.: Particle scattering, backscattering, and absorption coefficients: An in situ closure and sensitivity study, J. Geophys. Res., 107, 8122, doi:10.1029/2000JD000234, 2002.

Table 1. Calculation of C according to Eq. (20) using C^* and m_s as given by Arnott et al. (2005). For ω_0 (521 nm) and a_s we assumed 0.92 and 2, respectively.

	C at various wavelengths (nm)							Ratios of C for two wavelengths			
a_a	370	470	521	590	660	880	950	660/470	950/470	521/470	950/521
1	2.355	2.656	2.677	2.730	2.827	2.933	2.925	1.065	1.102	1.008	1.093
1.5	2.270	2.626	2.677	2.770	2.909	3.144	3.179	1.107	1.211	1.019	1.187
2	2.198	2.599	2.677	2.812	3.000	3.420	3.523	1.15	1.356	1.030	1.316

ACPD
5, 9355–9404, 2005

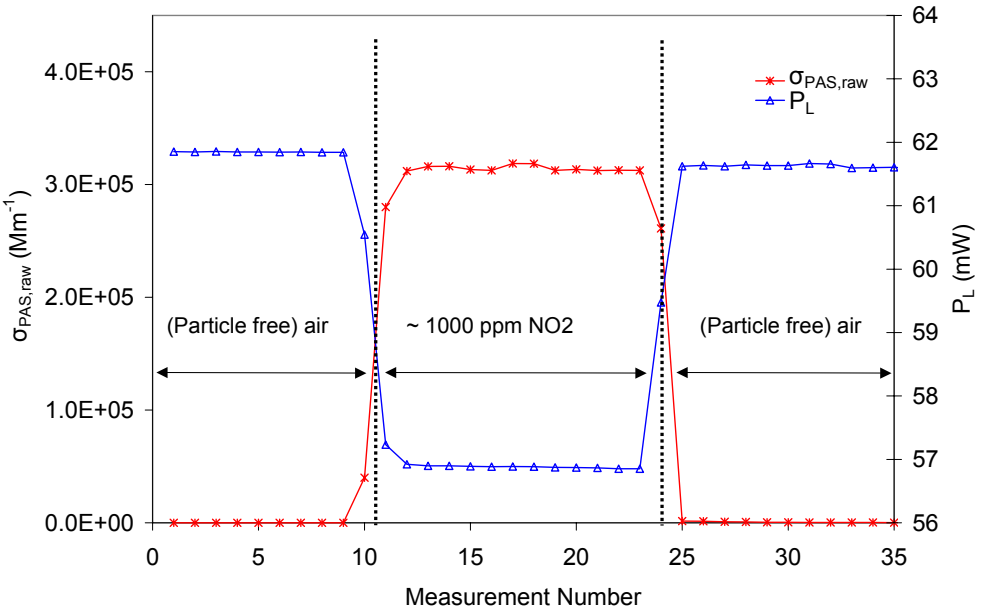

Fig. 1. Response of the PAS during a NO_2 calibration cycle, where $\sigma_{PAS,raw}$ (stars) and P_L (triangles) are the photoacoustically determined absorption coefficient and the laser power, respectively.

ACPD
5, 9355–9404, 2005

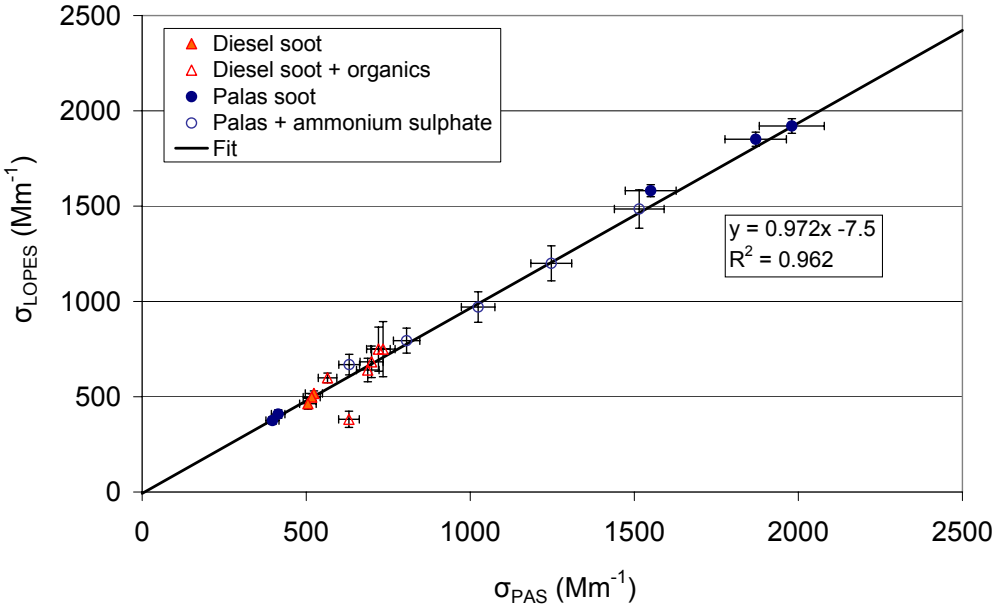

Fig. 2. Comparison of absorption coefficients determined by the PAS and an optical extinction cell (LOPES) for both pure soot (Diesel and spark-generated (Palas) soot) and coated soot particles (internally mixed aerosols).

ACPD
5, 9355–9404, 2005

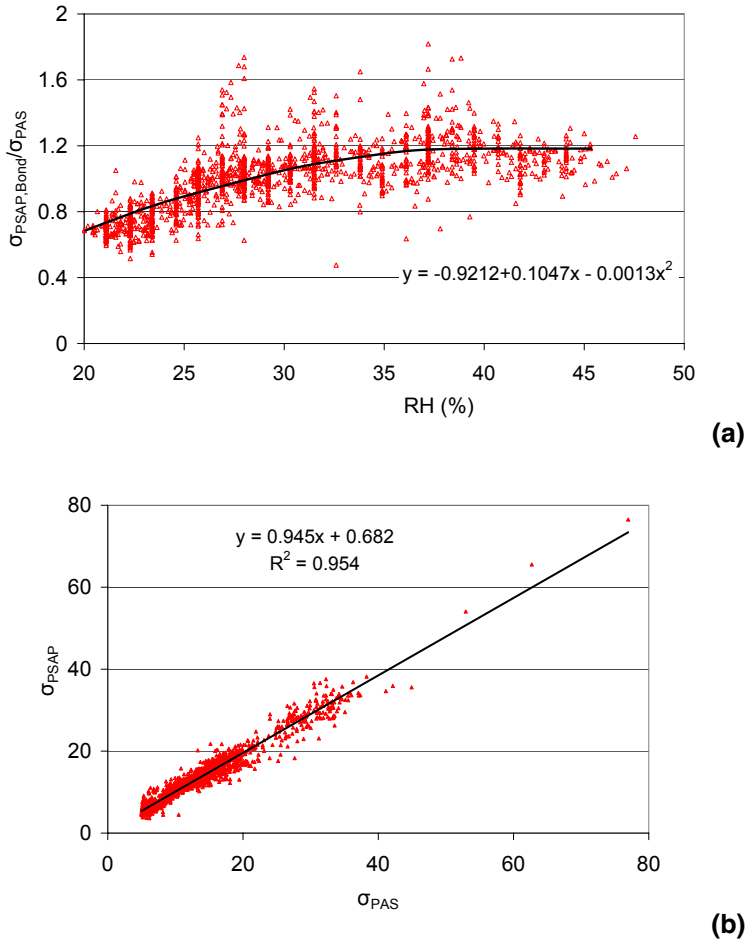

Fig. 3. (a) Dependence of the Bond corrected normalized PSAP absorption coefficient on RH. **(b)** Correlation of σ_{PSAP} the Bond and RH corrected PSAP absorption coefficient with σ_{PAS}.

ACPD
5, 9355–9404, 2005

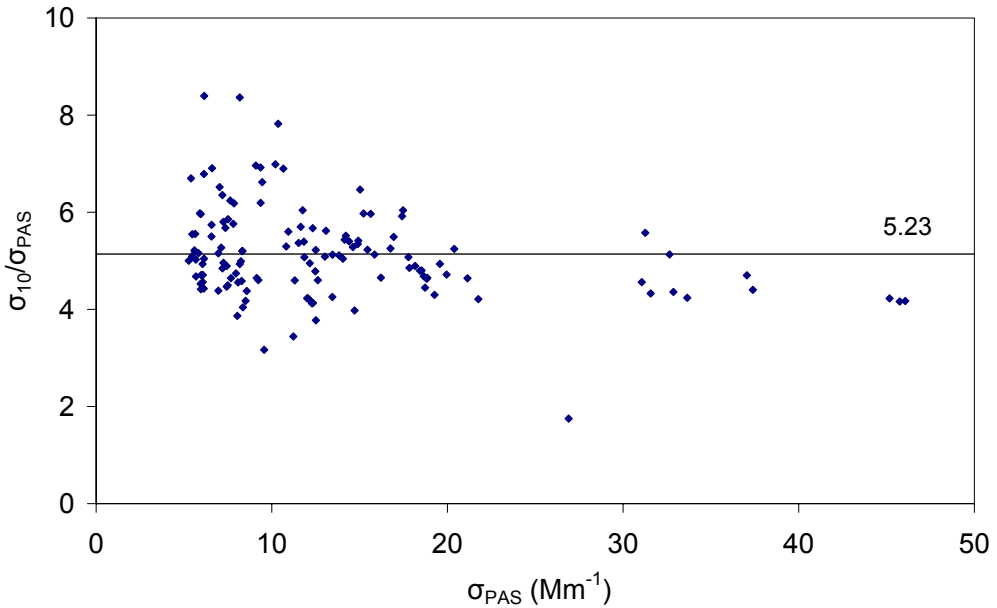

Fig. 4. Experimental determination of the multiple scattering factor C for the Aethalometer according to Eq. (11). The solid line represents the arithmetic mean (=5.23) of the ratio of σ_{10} and σ_{PAS} at 532 nm.

ACPD
5, 9355–9404, 2005

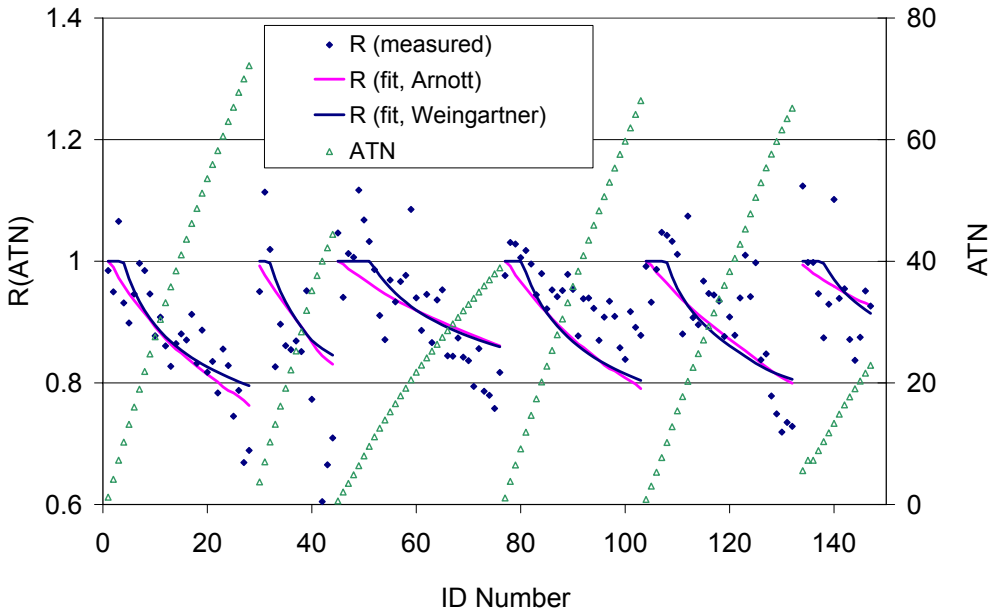

Fig. 5. Illustration of the decreasing Aethalometer sensitivity (R) with increasing filter loading (ATN, open triangles). The measured sensitivity (solid diamonds) was fitted according to the expressions provided by Weingarter et al. (2003) (blue line) and Arnott et al. (2005) (magenta line).

ACPD
5, 9355–9404, 2005

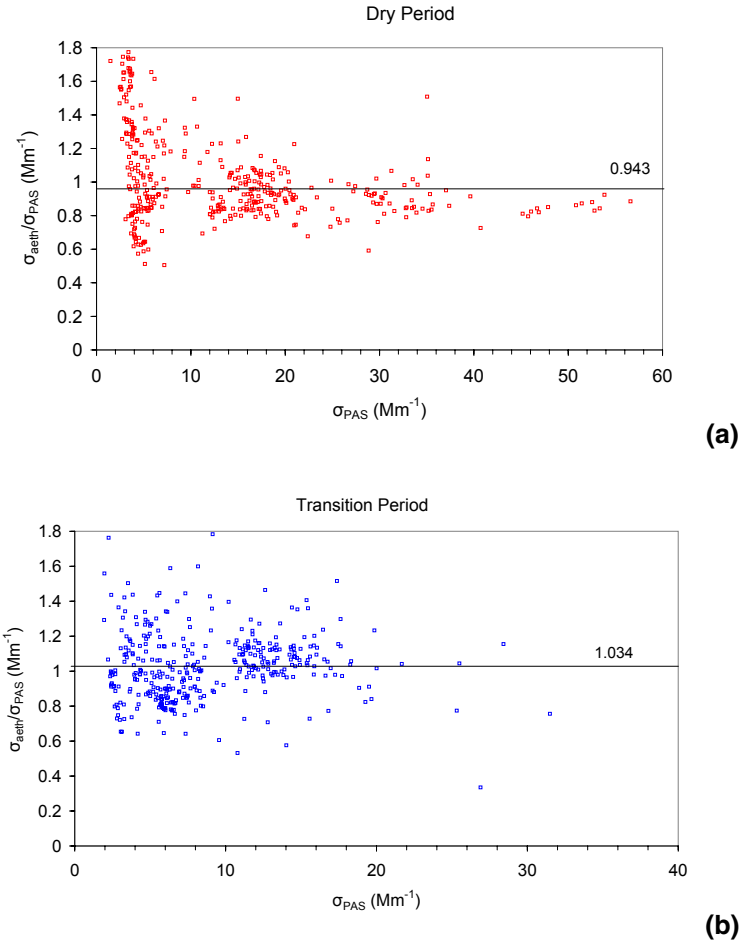

Fig. 6. Dependence of the normalized corrected Aethalometer data on pollution level (represented by σ_{PAS}) and sampling season, namely the dry **(a)** and transition period **(b)**.

ACPD
5, 9355–9404, 2005

Field calibration of aerosol absorption measurement techniques

O. Schmid et al.

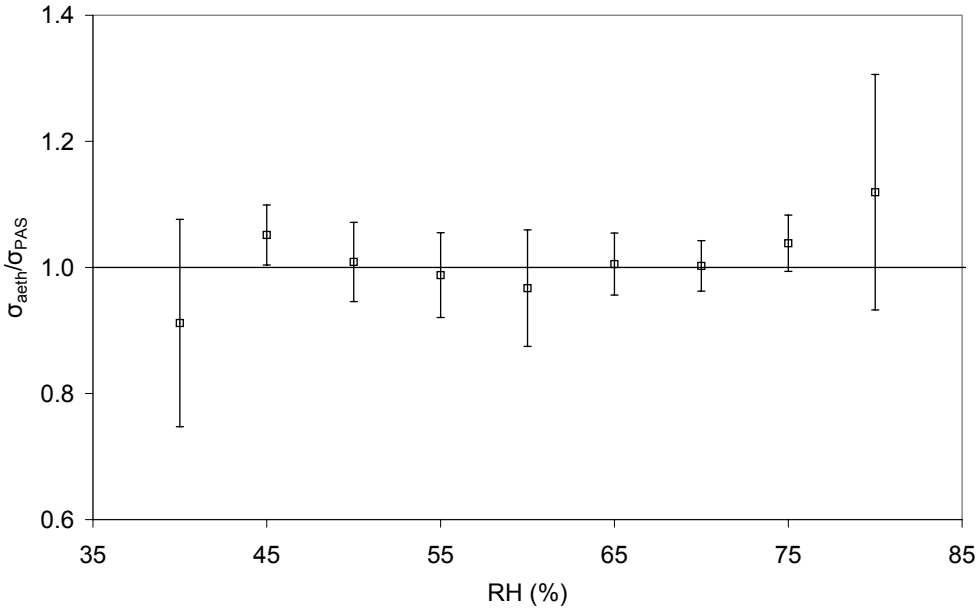

Fig. 7. The effect of relative humidity (RH) on Aethalometer performance. Depicted are the mean and 95% confidence level of the ratios of ambient and dry absorption coefficients as measured by the Aethalometer (σ_{aeth}) and the photoacoustic spectrometer (σ_{PAS}), respectively.

ACPD
5, 9355–9404, 2005

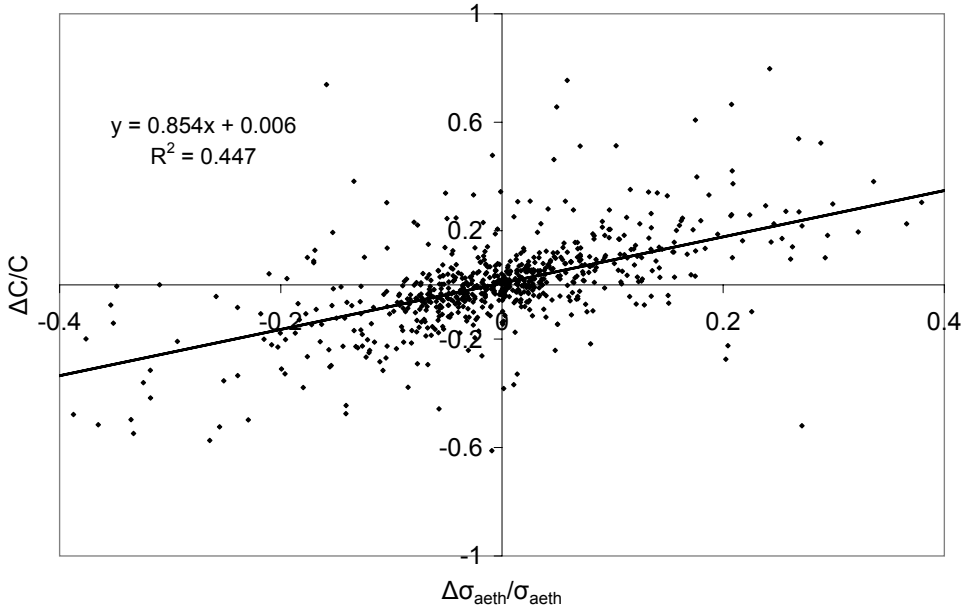

Fig. 8. The positive correlation between changing pollution level ($\Delta\sigma_{aeth}/\sigma_{aeth}$) and Aethalometer signal ($\Delta C/C$) suggests that gaseous adsorption has a measurable effect on the Aethalometer performance.

ACPD
5, 9355–9404, 2005

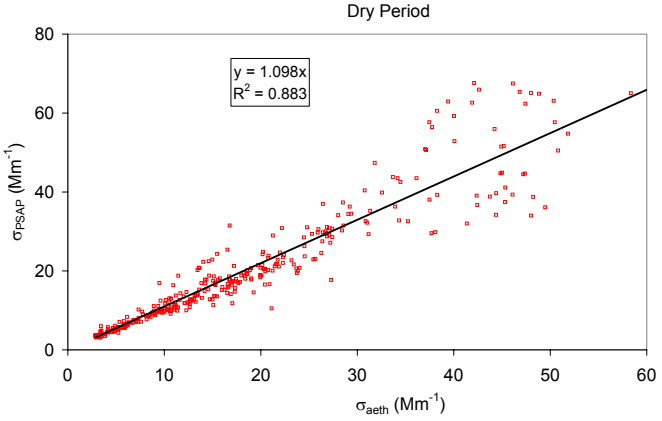

(a)

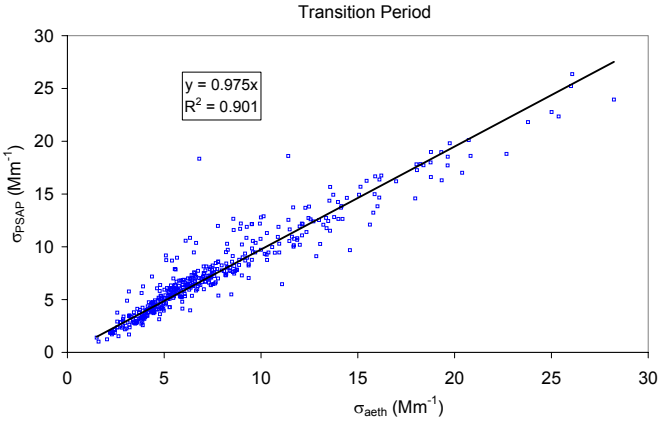

(b)

Fig. 9. Comparison of the absorption coefficients (at 532) measured by PSAP and Aethalometer for both the dry **(a)** and transition period **(b)**.

ACPD

5, 9355–9404, 2005